ELECTRONIC AND VIBRATIONAL SPECTROSCOPY OF $Ni^+(H_2O)$

A Thesis Presented

by

JENNIFER S. DALUZ

Submitted to the Graduate School of the
University of Massachusetts Amherst in partial fulfillment
of the requirements for the degree of

Master of Science

May 2011

Chemistry Graduate Program

© Copyright by Jennifer Daluz 2011
All Rights Reserved

ELECTRONIC AND VIBRATIONAL SPECTROSCOPY OF $Ni^+(H_2O)$

A Thesis Presented

by

JENNIFER S. DALUZ

Approved as to style and content by:

Ricardo B. Metz, Chair

Justin Fermann, Member

Craig Martin, Department Head
Department of Chemistry

DEDICATION

To all the panda bears that have been suffering because of climate change, and to my supporting family and friends.

ACKNOWLEDGMENTS

I would especially like to thank my advisor, Ricardo B. Metz, for his patience and continuous support. I would also like to thank my group members for making this time enjoyable. I also extend my gratitude to my committee member Professor Justin Fermann for having thoughtful suggestions and comments.

I would like to thank all my friends, particularly Jovana Golijanin for all the inspiration and praise.

ABSTRACT

ELECTRONIC AND VIBRATIONAL SPECTROSCOPY OF $Ni^+(H_2O)$

MAY 2011

JENNIFER DALUZ, B.S., UNIVERSITY OF MASSACHUSETTS AMHERST

M.S., UNIVERSITY OF MASSACHUSETTS AMHERST

Directed by: Ricardo B. Metz

The electronic and vibrational spectra of $Ni^+(H_2O)$ were measured using photofragment spectroscopy. In the electronic spectrum, photodissociation is observed at photon energies above 16875 cm^{-1}. The only fragment observed is Ni^+. The electronic spectrum consists of well-resolved peaks spaced by ~340 cm^{-1}, due to a vibrational progression in the excited electronic state. These peaks have complex sub-structure, consisting of a triplet, spaced by ~30 cm^{-1}. The sub-structure is due to rotational structure in a perpendicular transition of a prolate top molecule. In addition to this major progression, there is a series of less intense, single peaks spaced by ~340 cm^{-1}. These may be due to a vibrational progression in a second electronic state, this time due to a parallel transition.

The O-H stretching vibrations of $Ni^+(H_2O)$ were measured using vibrationally mediated photodissociation (VMP) in a depletion experiment, only monitoring transitions from K''=1. This revealed a O-H symmetric stretch at 3629 cm^{-1} and antisymmetric O-H stretch at 3692 cm^{-1}.

Several electronic structure calculations complement the experiments using the BHandHLYP hybrid density functional and the 6-311++G(3dp, f) basis set. At this level of theory, $Ni^+(H_2O)$ is predicted to have C_{2v} symmetry and $^2A_1$ ground state. The Ni-O

bond length is 1.95, the O-H bond lengths are .955 and the H-O-H angle is 108.2° The molecule is a near-prolate top, with rotational constants A=13.98 cm^{-1}, B=0.297 cm^{-1} and C=0.296 cm^{-1} . Analysis of the electronic and vibrational spectra reveals that binding to Ni^+ removes electron density from the oxygen lone pairs, increasing the H-O-H bond angle from its value in bare H_2O. The electronic and vibrational spectra corresponds to 4s ←3d transistion in Ni^+. As a result of electronic excitation, the Ni-O bond stretches by .20 Å, and the H-O-H bond angle is reduced.

TABLE OF CONTENTS

ACKNOWLEDGMENTS v

ABSTRACT vi

LIST OF TABLES ix

LIST OF FIGURES x

CHAPTER

1. INTRODUCTION 1

    1.1 Motivation 1

    1.2 Background 1

2. EXPERIMENTAL METHOD 3

    2.1 Photofragment Spectroscopy 3

    2.2 Vibrationally Mediated Photodissociation 4

    2.3 Experimental Details 5

3. RESULTS 8

4. ANALYSIS AND DISCUSSION 13

    4.1 Vibrational and Rotational Analysis of Ground State 13

    4.2 Electronic Spectroscopy-Vibrational Structure 19

    4.3 Electronic Spectroscopy-Rotational Structure 26

5. SUMMARY AND CONCLUSIONS 30

6. FUTURE WORK 31

BIBLIOGRAPHY 32

LIST OF TABLES

Table Page

Table 1. Calculated and Experimental $Ni^+(H_2O)$ Stretching and Bending Frequencies 15

Table 2. Calculated O-H Bond Length and H-O-H Bond Angle 15

Table 3. Spectroscopic Constants and Dissociation for $Ni^+(H_2O)$ 20

Table 4. Experimental and Calculated Ni-O Bond Lengths for the Ground (Ni^+-O) and Excited (Ni^{+*}-O) States 26

Table 5. Rotational Constants for the Ground and Excited Electronic States of $Ni^+(H_2O)$ 29

LIST OF FIGURES

Figure Page

Figure 1. A Representation of the Dual-Time of Flight Mass Spectrometer Used in This Study 7

Figure 2. Electronic Spectrum of $Ni^+(H_2O)$ Measured Using Photofragment Spectroscopy..... 10

Figure 3. Vibrational Spectrum of $Ni^+(H_2O)$ 11

Figure 4. Rotational Simulation in the Vibrational Spectrum of $Ni^+(H_2O)$ 17

Figure 5. $Ni^+(H_2O)$ Ground State, 5th and 6th Excited State and Respective Potential Energy Surfaces..... 22

Figure 6a. Calculated Potential Energy Surface 23

Figure 6b. Orbital Diagram of Expected Transition 24

Figure 7. Rotational Simulation in the Electronic Spectrum 27

CHAPTER 1

INTRODUCTION

1.1 Motivation

Noncovalent interactions are key to molecular recognition and higher-order structure in biological systems. Metal-H_2O binding is important in several enzymes. Urease catalyzes the reaction of urea with water to form carbon dioxide and ammonia. It has two nickels at the active site, one of which is coordinated to H_2O.[1] In the proposed mechanism, this water is deprotonated and subsequently reacts with the urea.[2] Noncovalent interactions are also key to ion solvation. Despite their non-covalent nature, ion-water bonds can be very strong, even for singly-charged ions. This thesis will examine Ni^+-H_2O interactions using spectroscopic techniques. It addresses several fundamental questions. How strongly does Ni^+ bind to H_2O? How is this affected by the electronic configuration of the metal? How does binding to the metal perturb the O-H bonds and the geometry of the H_2O, particularly the H-O-H bond angle?

1.2 Background

There have been have been a few previous studies investigating non-covalent Ni^+ complexes in the gas phase. Dalleska et al. used guided ion beam methods to measure binding energies of the first four H_2O molecules to the first row transition metal ions M^+.[3,4] They find binding energies to be 15100 cm^{-1}, 14060 cm^{-1}, 5650 cm^{-1}, and 4300 cm^{-1} for $Ni^+(H_2O)_n$, n=1-4, respectively. Brucat and co-workers have measured electronic spectra of complexes of Ni^+ with Ar, N_2O, and CO_2 using photofragment spectroscopy.[5-8] They determined binding energies, and in some cases, vibrational frequencies. Walter et al. have measured vibrational spectra of $Ni^+(H_2O)_n$ clusters, n=1-25, in the O-H

stretching region through means of IR photofragment spectroscopy.[9] Because the energy required to break the $Ni^+(H_2O)_n$ bond is greater than that available with one IR photon for n=1-4, they studied $Ni^+(H_2O)_n(Ar)_m$ instead, monitoring absorption via argon loss. It is possible that the argon tag may perturb the O-H stretches. In addition, the rotational structure of $Ni^+(H_2O)(Ar)_2$, the smallest cluster studied, is very different from that of $Ni^+(H_2O)$. My current study is a direct analysis of gas phase $Ni^+(H_2O)$ using electronic and vibrational spectroscopy, measured via photofragment spectroscopy. With spectroscopy as a tool I have probed questions like how strongly does Ni^+ bind to H_2O and how this is affected by the Ni^+ electronic configuration. By studying the vibrational structure of the complex I have determined how binding to the Ni^+ perturbs the O-H bonds and the geometry of the H_2O, particularly the H-O-H bond angle.

CHAPTER 2

EXPERIMENTAL METHOD

2.1 Photofragment Spectroscopy

The concentration of $Ni^+(H_2O)$ in this study is too low to permit direct absorption measurement of its vibrational and electronic spectra. Instead, spectra are measured indirectly, using photofragment spectroscopy. In photofragment spectroscopy the molecule of interest absorbs one or more photons with enough energy to break a bond. Depending on the potential energy surface (PES), the molecule may completely dissociate in a time period that is shorter than needed to observe molecular vibrations, this process is known as direct dissociation. The molecule may also go through predissociation, in which case the dissociation occurs slowly enough for vibrations or even rotations to be observed, typically a result of the molecule becoming trapped in a well of the PES, and only dissociating as a result of internal conversion. Predissociation reveals important vibrational and rotational information about the molecule, and is the basis for photodissociation spectroscopy.

A photodissociation spectrum is compiled by scanning a dissociation laser over a spectral region and monitoring parent fragment ion yields. Photodissociation requires that the molecule absorb light and dissociate. The photodissociation spectrum is thus the product of the absorption spectrum and photodissociation quantum yield.

For $Ni^+(H_2O)$, which has a Ni^+-H_2O bond strength[3,4] of 1.87±0.03 eV (15100 ± 200 cm^{-1}) , one photon with a wavelength λ<662 nm has sufficient energy to dissociate the molecule. Thus, the electronic spectrum in the visible or ultraviolet can be conveniently measured using photofragment spectroscopy. However, one IR photon in

the O-H stretching region, near 3700 cm^{-1} has ~ 0.46 eV of energy, so at least four IR photons are required for dissociation. From the photodissociation spectrum, questions regarding vibrational frequencies, rotational constants, bond dissociation energies, PES of upper states, and upper state lifetimes and how they are affected by excitation energy can all be answered.

2.2 Vibrationally Mediated Photodisoociation (VMP)

A technique used to study vibrational spectra of gas-phase molecules is vibrationally mediated photodissociation (VMP).[10] VMP is particularly good for measuring vibrational spectra of small, tightly bound molecules, such as $Ni^{+}(H_2O)$ [11]. The success of VMP hinges on the photodissociation spectrum of vibrationally excited molecules differing from that of ground state molecules. It can be carried out in enhancement or depletion mode. In an enhancement experiment, a visible or UV laser is set to a wavelength were vibrationally excited molecules (but not ground state molecules) absorb light, undergo an electronic transition and dissociate. As an IR laser is scanned, photofragments are only observed when it is in resonance with a vibration in the molecule. This requires knowing the electronic transition wavelengths for vibrationally excited molecules. The depletion experiment is more general, but has much larger background. A visible or UV laser is tuned to an electronic transition of ground state molecules, leading to photodissociation. An IR laser is then scanned. When it comes into resonance with a vibration, it depletes the molecules' ground state population, reducing the amount of photodissociation. This is why this technique is referred to as a depletion experiment.

2.3 Experimental Details

The experiment takes place in a dual time-of-flight mass spectrometer, whose setup is illustrated in Figure 1. First, a Continuum Minilite laser (A), operating at 20 Hz ablates a rotating nickel rod (B), forming metal ions. The nickel ions then interact with the ~20 psi of backing gas that is introduced by a piezo-electric valve, which is also operating at 20 Hz (C). The backing gas consist of a precursor, H_2O that is diluted to ~ 0.14% in either a He or Ar carrier gas. The purpose of the carrier gas is to vibrationally cool the molecule through collisions. The molecules expand into vacuum, cooling to rotational temperatures of 5-20 K.

The metal complexes then pass through a skimmer (D) into the acceleration region, where they are accelerated using two electric fields (E).[12] In this region there are three plates; the first is the pulsed extraction plate, the second is grounded, and third is the acceleration plate. The first plate is pulsed from ground to 100V as the ions enter. The acceleration plate has a constant voltage of -1800V. When the extraction plate is pulsed, only the ions between the first two plates accelerate onward. The ions that are closest to the pulsed plate will end up with nearly 1900 V of kinetic energy (KE) and the ions closer to the ground plate will have about 1800V of KE. This difference in KE is enough to compensate for the molecules' different starting points, so they arrive at the point of dissociation at the same time. After accelerating, the ion beam is re-referenced to ground potential (F). At this point, the beam proceeds through the Einzel Lens (G) where they are focused and then deflectors (H) direct them into the mass gate (I). The mass gate is pulsed so that only the mass-selected ions of interest enter the reflectron (K). The purpose of the reflectron is to give the parents and fragments different flight times,

so they can be selectively detected. The ions are dissociated at the turning point of the reflectron by either a dye laser or an IR laser system, producing fragmentation (J). The dye laser is a Continuum ND60, pumped by a Continuum Surelite I-20 Nd:YAG laser. It produces >10 mJ/pulse and is tunable from 545 to ~800 nm with a line width of 0.1 cm^{-1}. The IR laser system is a LaserVision OPO/OPA pumped by a Continuum Powerlite 8020. It is tunable from 2200 to >4000 cm^{-1} and produces ~12 mJ/pulse near 3700 cm^{-1}. In the VMP experiments the IR laser fires 40 ns before the visible laser. Finally, the ions reach the 40 mm dual microchannel plate (MCP) detector (L). When a particle encounters the surface of the detector, electrons are expelled and accelerated down the channel by a bias voltage. This technique results in 10^6 electrons traveling down the channel per surface contact. The electrons are then conducted to ground using a 50 Ω resistor, creating a voltage pulse that is later amplified, resulting in a 10 mV, 5 ns pulse for each ion. The resulting signal is collected using a gated integrator and a LabView based program.

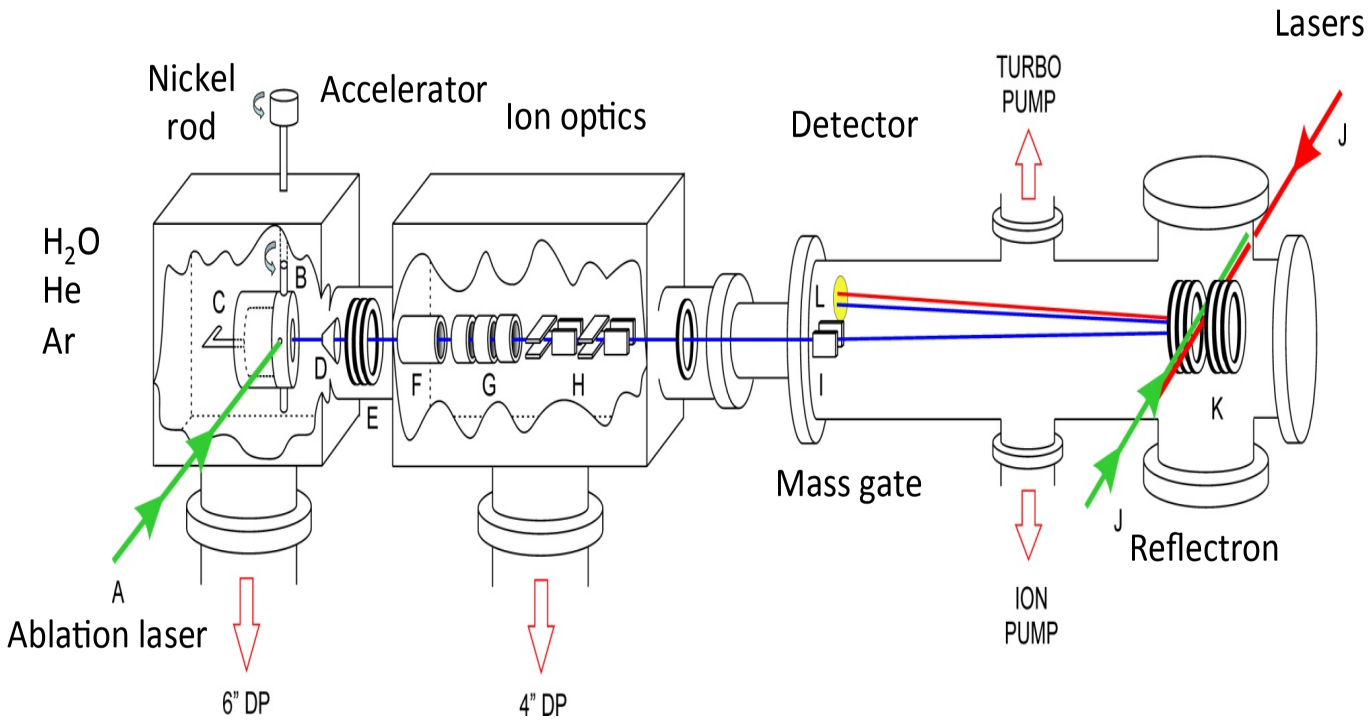

Figure 1.

A representation of the dual time-of-flight mass spectrometer used in this study. The ablation laser (A) irradiates a Ni rod (B). The backing gas of He and .03% H_2O is pulsed into the first chamber using a piezo-electric valve (C). The $Ni^+(H_2O)$ complexes are formed, cooled by expansion into vacuum and pass through the skimmer (D) and passes through the acceleration region (E). The ions are re-referenced to ground potential (F) and focused through the Einzel Lens (G) and are directed by deflectors (H) into the mass gate (I). The mass selected ions travel to the reflectron (K) where they are photodissocated at the turning point by the visible and IR lasers (J). Finally the fragments reach the dual-microchannel plate detector (L).

CHAPTER 3

RESULTS

The electronic and vibrational spectra of $Ni^+(H_2O)$ were measured using photofragment spectroscopy. In the electronic spectrum, photodissociation is observed at photon energies above 16875 cm^{-1}. The only fragment observed is Ni^+. Although nickel has several naturally occurring isotopes, all the data obtained are for the major isotope, ^{58}Ni (68% natural abundance). The photodissociation spectrum is shown in Figure 2. It consists of well-resolved peaks spaced by ~340 cm^{-1}, due to a vibrational progression in the excited electronic state. These peaks have complex sub-structure, consisting of a triplet, spaced by ~30 cm^{-1}. As will be discussed in detail below, the sub-structure is due to rotational structure in a perpendicular transition of a prolate top molecule. In order of increasing energy, the three transitions correspond to K'=0←K''=1, K'=1←K''=0 and K'=2←K''=0, where K is the quantum number for rotation about the *a* axis (the Ni-O bond). In addition to this major progression, there is a series of less intense, single peaks spaced by ~340 cm^{-1}. These may be due to a vibrational progression in a second electronic state, this time due to a parallel transition.

The O-H stretching vibrations of $Ni^+(H_2O)$ were measured using vibrationally mediated photodissociation in a depletion experiment. We set the visible laser to the $v'_{Ni\text{-}O}$ =1, K'=2 ← $v''_{Ni\text{-}O}$ =1, K''=1 transition at 17257 cm^{-1}. We then scan the IR laser, which fires befor the visible laser. When this laser is resonant with a vibrational transition such as the OH antisymmetric stretch, some molecules are vibrationally excited, which removes population from the ground state. This will lead to less

photodissociation (*if vibrationally excited moleucules are less likely to photodissociate than ground state molecules*).

When the visible laser is set to the K'=2←K''=1 transition at 17257 cm^{-1}, a depletion experiment monitors transitions from K''=1 only. The resulting spectrum obtained by scanning the IR laser is shown in Figure 3. In a second depletion experiment, transitions from K''=0 were monitored by setting the visible laser to the K'=1←K''=0 transition at 17223 cm^{-1} and scanning the IR laser.

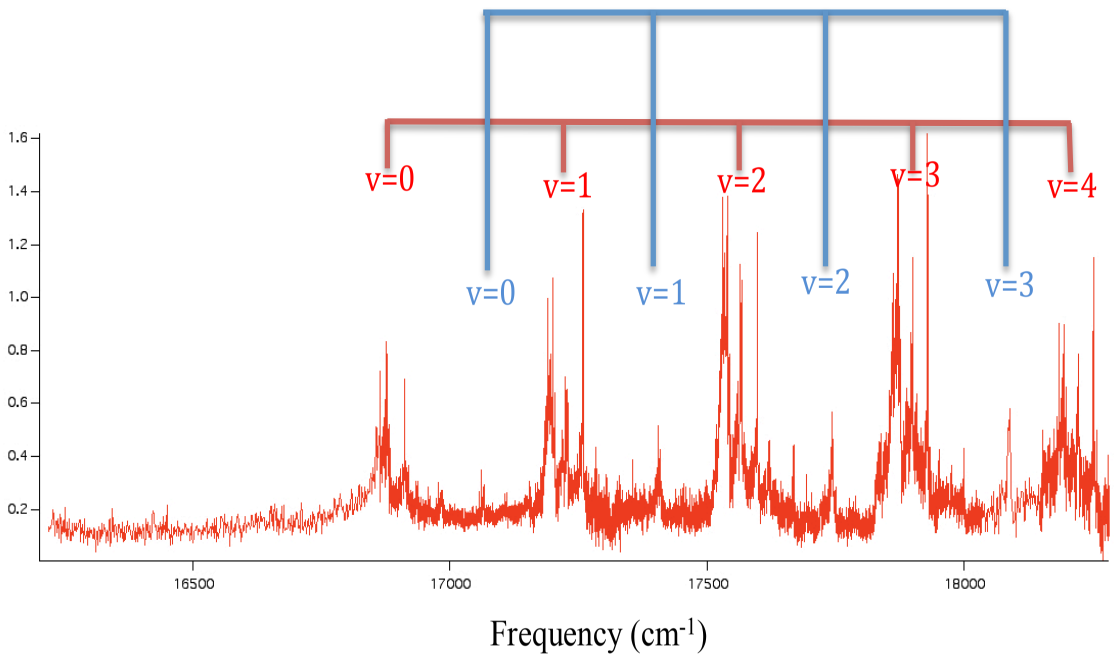

Figure 2.

The electronic spectrum of $Ni^+(H_2O)$ measured using photofragment spectroscopy. 16863cm^{-1} is the photodissociation onset, the Ni^+-O stretch was measured to be 340cm^{-1}. A series of perpendicular bands, labeled with quantum numbers v (red) are observed. There are also a series of bands that are indicated with blue combs but are not labeled. These peaks are expected to be vibrational progressions in the electronic spectrum of the 6th excited state in another electronic state.

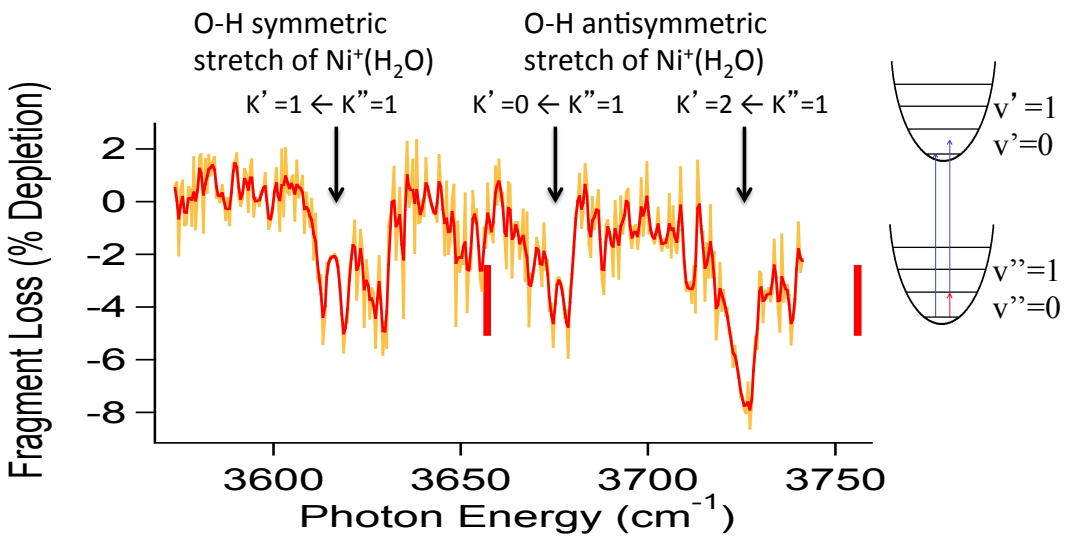

Figure 3.

Vibrational Spectrum of $Ni^+(H_2O)$. The O-H stretching frequencies in $Ni^+(H_2O)$ were measured using vibrationally mediated photodissociation with the visible laser set to the (v'=1,K'=2 ←v"=0,K"=1) line at 17257 cm^{-1}.

Several electronic structure calculations complement the experiments. The calculations employ the BHandHLYP hybrid density functional and the 6-311++G(3dp, f) basis set. The geometry of $Ni^+(H_2O)$ was calculated, along with its vibrational frequencies. In addition, time-dependent density functional theory (TD-DFT) was used to characterize excited electronic states of $Ni^+(H_2O)$. This functional was selected because it accurately describes the excitation energies of electronic states of Ni^+ in the visible region of the spectrum. At this level of theory, $Ni^+(H_2O)$ is predicted to have C_{2v} symmetry and $^2A_1$ ground state. The Ni-O bond length is 1.95 Å, the O-H bond lengths are 0.955 Å and the H-O-H angle is 108.2˚. The molecule is a near-prolate top, with rotational constants A=13.98 cm^{-1}, B=0.297 cm^{-1} and C=0.296 cm^{-1} (a perfect prolate top has A>B and B=C). The A constant is much larger than B or C, as it is due to rotations about the Ni-O axis (the *a* axis). This has very small moment of inertia, as the H atoms are the only atoms not on this axis. Rotation about the *b* and *c* axes has much larger moment of inertia, as the Ni and O do not lie on these axes and thus contribute to the moment of inertia.

CHAPTER 4

ANALYSIS AND DISCUSSION

4.1 Vibrational and Rotational Analysis of Ground State

Vibrationally mediated photodissociation was used to probe the O-H stretching vibrations in the ground electronic state of $Ni^+(H_2O)$ in a depletion experiment. The $Ni^+(H_2O)$ ion is a symmetric prolate top, and the major progression observed in the electronic spectrum is a perpendicular transition, with the transition moment perpendicular to the *a* axis (the Ni-O bond). The selection rules for a perpendicular band are $\Delta K=\pm1$ and $\Delta J=0, \pm1$, which can be seen in the photodissociation spectrum of the molecule, shown in Figure 2.

Vibrational spectra were measured using VMP and two different rotational transitions in the electronic spectrum. The visible laser was first set to the K'=2←K''=1 transition at 17257 cm^{-1}. Scanning the IR laser in a depletion experiment then monitors transitions from K''=1 only. The resulting spectrum is shown in Figure 3. In the vibrational spectrum, the O-H symmetric stretch (v_{ss}) is a parallel transition, with the selection rules $\Delta K=0$ and $\Delta J=\pm1$. The $v_{ss}'=1$, K'=1← $v_{ss}''=0$,K''=1 transition is observed at 3629 cm^{-1}. The O-H antisymmetric stretch (v_{as}) is a perpendicular transition. Two absorptions are observed: $v_{as}'=1$, K'=0← $v_{as}''=0$,K''=1 at 3678 cm^{-1} and $v_{as}'=1$, K'=2← $v_{as}''=0$, K''=1 at 3727 cm^{-1}.

In order to get a more complete understanding of the vibrational states, a second depletion experiment was performed with the visible laser stationed at the K'=1←K''=0 transition at 17223 cm^{-1}. The second depletion experiment revealed the $v_{as}'=1$, K'=1← $v_{as}''=0$, K''=0 transition at 3689 cm^{-1}.

Table 1 lists the vibrational frequencies and descriptions for bare H_2O and $Ni^+(H_2O)$. It can be noted that the addition of Ni^+ to the H_2O causes a red shift in the O-H stretches. The symmetric O-H stretch shifts ~30 cm^{-1} and the antisymmetric O-H stretch is shifted by 78 cm^{-1}. For comparative purposes a theoretical study of the $Ni^+(H_2O)$ system was also performed using Gaussian03 and Gaussian09 at the BHandHLYP/6-311++G(3df,p) and B3LYP/6-311++G(3df,p) levels. All pertinent stretches and frequencies that will be henceforth be referred to are summarized in Table 1. The calculated harmonic frequencies are scaled by 0.96 (B3LYP) and 0.92 (BHandHLYP) to match the experimental O-H stretches in bare H_2O. The calculations predict that binding to Ni^+ produces a red shift of 53 cm^{-1} for the symmetric and 74 cm^{-1} for the antisymmetric stretch, in good agreement with the experiment. The red shifts can be explained in terms of inductive effects. Upon complexation, the Ni^+ atom removes electron density from the oxygen lone pair in H_2O, weakening the O-H bonds and increasing the H-O-H bond angle. This effect has been observed for many $M^+(H_2O)$ complexes, including the $Cr^+(H_2O)Ar$[13] and $Ni^+(H_2O)(Ar)_2$[9], and $Co^+(H_2O)$[14] systems done by the Duncan and Metz groups, respectively.

Description	Frequency (cm^{-1}) $Ni^+(H_2O)$ Calculated	Frequency (cm^{-1}) $Ni^+(H_2O)$ Experimental	Frequency (cm^{-1}) H_2O
H-O-H Symmetric Stretch	3610	3629	3657
H-O-H Antisymmetric Stretch	3681	3692	3756
H-O-H bend	1575	----	1595
In-Plane Bend	554	----	----
Ni-O Stretch	388	----	----
Out-Plane Bend	200	----	----

Table 1.

Calculated and experimental $Ni^+(H_2O)$ stretching and bending frequencies. The frequencies were calculated using BHandHLYP/6-311G++(3df,p). The bare H_2O frequencies are also listed. The experimental $Ni^+(H_2O)$ frequencies red shift for the symmetric and antisymmetric stretches ~30 cm^{-1} and ~80 cm^{-1}, respectively, relative to bare H_2O. Calculated frequencies are scaled by .92

This effect is also observed in the calculations, tabulated in Table 2. The inductive effect can be seen in the calculated values for the O-H bond length and H-O-H bond angle. Using the BHandHLYP/6-311++G(3df,p) functional, the O-H bond length and H-O-H bond angle of bare H_2O were calculated to be .950 Å and 105.9º, respectively. Binding to Ni^+ is predicted to increase the O-H bond length by .005 Å and the H-O-H angle by 2.3º.

	$Ni^+(H_2O)$	H_2O
O-H Bond Length (Å)	.955 Å	.9504 Å
H-O-H Bond Angle	108.2˚	105.9˚

Table 2.

Calculated O-H bond length and H-O-H bond angle. Calculated geometries were determined using BHandHLYP/6-311++G(3df,p)

DFT calculations using the BHandHLYP functional predict that the ground rotational A constant, A'' = 13.98 cm^{-1}. Using this as an original parameter, the rotational structure in the vibrational spectrum was fit using the spfit and spcat

programs.[15] The rotational fit, Figure 4, of the vibrational spectrum revealed that the A'' constant was actually 13.58 cm^{-1}, which is in excellent agreement with the calculated value. Because this molecule is a prolate top it can be expected that the rotational constants B'' and C'' are equal. The B'' and C'' constants were predicted to be 0.297 cm^{-1} and 0.296 cm^{-1}, respectively.

The rotational simulation of the vibrational spectrum in Figure 4 consists of three peaks, the symmetric stretch and two antisymmetric stretches. The symmetric peak located at 3627 cm^{-1} is a parallel band rising from K'=1←K''=1,and because it is a parallel band the only information it yields is the rotational temperature. Changing different parameters for the symmetric stretch showed that this band is sensitive to the J rotational temperature and is insensitive to changes in the A' constant and spin rotation constant ε.

From the fit, the rotational temperature is 20 K. The two antisymmetric absorptions at 3678 cm^{-1} and 3627 cm^{-1} are also informative. Because $Ni^{+}(H_2O)$ is a prolate top, the energy of a state with quantum numbers J and K is given by Equation 1. The splitting between states with K=0 and K=2 is given by Equation 2, which can be employed to determine the rotational constant A.

Equation 1: $E_{J,K} = \left(A - \frac{B+C}{2}\right)K^2 + \left(\frac{B+C}{2}\right)J(J+1)$

Equation 2: $E_{J,K=2} - E_{J,K=0} = 4(A - \left(\frac{B+C}{2}\right))$

The rotational simulation for the vibrational structure determined the rotational temperature and the A rotational constants for the ground electronic states as well as the accurate antisymmetric stretch frequency, 3692 cm^{-1}. The values found in this simulation can then be used to model the rotational structure in the electronic spectrum.

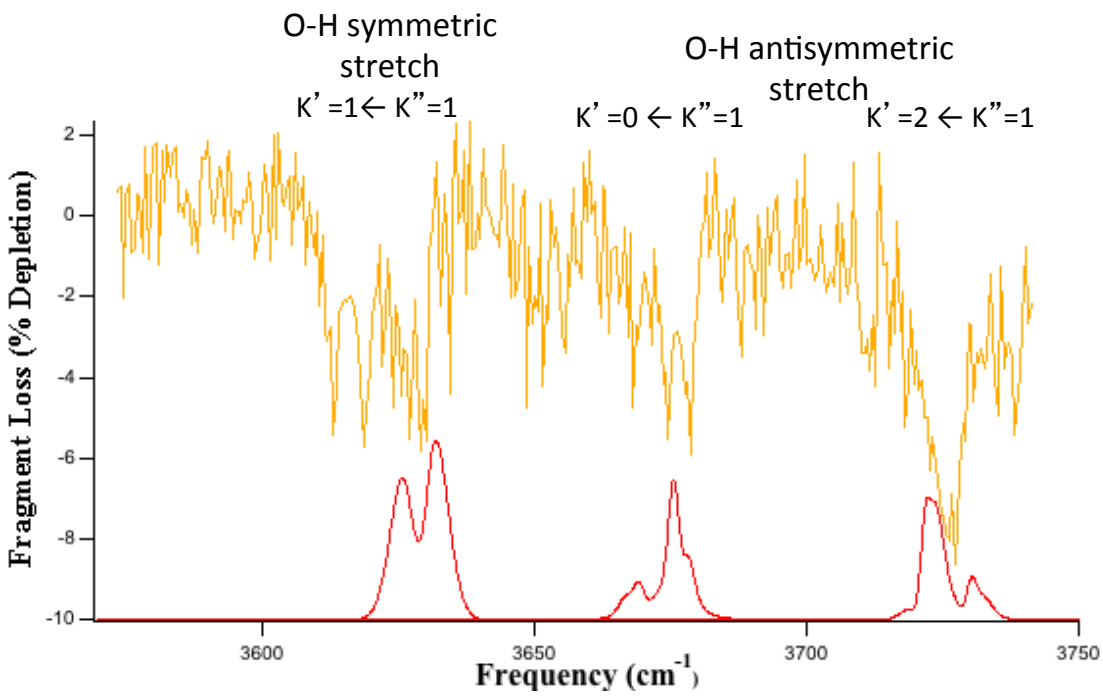

Figure 4.

Rotational simulation in the vibrational spectrum of $Ni^+(H_2O)$. The vibrational spectrum is in the O-H stretching region of $Ni^+(H_2O)$. The upper, yellow trace is obtained by setting the visible laser to the v'=1,K'=2 ←v"=0,K"=1 band in the electronic spectrum at 17257 cm^{-1} and monitoring fragment signal while scanning the IR Laser in VMP depletion experiment. The lower red trace is a rotational simulation to the vibrational spectrum. The simulation was generated using spfit and spcat and illustrates the rotational structure in the vibrational spectra.[15]

Duncan and coworkers have studied the vibrational spectroscopy of $Ni^+(H_2O)Ar_2$, and complemented those studies with DFT calculations.[9] Experimentally, they have determined O-H the symmetric stretch to be 3623 cm^{-1}, which is in excellent agreement with the value of 3627 cm^{-1} obtained in this study. Their antisymmetric stretch frequency is also in excellent agreement. Duncan and coworkers determined it to be 3696 cm^{-1} and the value found in this study is 3692 cm^{-1}. Duncan and coworkers performed DFT calculations at the B3LYP/6-311+G** level and determined that the ground state of $Ni^+(H_2O)$ is a $^2B_2$ state with a Ni^+-O bond length of 2.002 Å. The ground state of $Ni^+(H_2O)$ in this study was found to be $^2A_1$ with a bond length of 1.952 Å. To determine which was the correct ground state, $Ni^+(H_2O)$ was recalculated using the B3LYP/6-311+G** functional. This calculation resulted in a $^2A_1$ state with a M^+-O bond length of 1.952 Å. Constraining the calculation to $^2B_2$ states gives a state 0.27 eV higher in energy with a Ni^+-O bond length of 2.002 Å. The ground state of Ni^+ is $3d^9$, ^2D. The lowest lying electronic states of $Ni^+(H_2O)$ also correspond to the $3d^9$ electron configuration of Ni^+. In the $^2A_1$ state, the orbital that is only singly occupied corresponds to the $3d_{z^2}$ orbital, which is oriented along the Ni-O bond. States with this orbital doubly occupied (such as the $^2B_2$ state) have more metal-ligand repulsion, which leads to higher energies and a longer Ni-O bond.

Other $M^+(H_2O)$ complexes that have been studied include $Co^+(H_2O)$ as done by Metz and coworkers. $Co^+(H_2O)$ is a particularly good comparison for the $Ni^+(H_2O)$ complex because it is also non-covalently bonded and Co^+ is very close to Ni^+ in chemical makeup. The $Co^+(H_2O)$ symmetric stretch was determined to be 3612 cm^{-1} and the antisymmetric stretch was 3692 cm^{-1}.[14]

4.2 Electronic Spectroscopy – Vibrational Structure

The photodissociation spectrum of $Ni^+(H_2O)$ starts at ~16840 cm^{-1} and consists of an extended progression of features spaced by ~340 cm^{-1}. Each feature consists of at least three peaks separated by ~30 cm^{-1}, characteristic of rotational structure from a prolate top with a large A constant of ~15 cm^{-1}. The first peak in the spectrum due to cold ions provides an upper limit the Ni^+-H_2O bond strength. The feature at 16840 cm^{-1} is due to transition from K''=1 to K'=0, so the transition at ~16875 cm^{-1}, corresponding to a transition from K''=0 to K'=1 prodives an upper limit to the Ni^+-H_2O bond strength of 2.092 eV. This upper limit is consistent with the guided ion beam study[3,4], which gives $D_O(Ni^+\text{-}H_2O)$ =1.87±0.03 eV. That the first observed peak lies well above the dissociation limit suggests that it is due to a transition to the ground vibrational state of the excited electronic state.

The vibrational frequency and anharmonicity are calculated using Equation 3.

Equation 3: $\Delta G(v') = E(v+1) - E(v) = w_e - 2(v+1)w_e x_e$

In Equation 3, $\Delta G(v')$ is the spacing between consecutive peaks, $w_e x_e$ is the anharmonicity constant in wavenumbers, w_e is the harmonic vibrational frequency also in wavenumbers, and v is the quantum number. The slope of this line is -2$w_e x_e$ and the D_0 can be found for $\Delta G(v') = 0$. The results are summarized in Table 3.

The excited state of $Ni^+(H_2O)$ accessed in this study correlates to electronically excited $Ni^{+*}+H_2O$. Which excited state is involved can be determined by estimating the adiabatic dissociation energy of the excited state. For a Morse oscillator,

Equation 4: $D_e(upper) = \frac{w_e^2}{4w_e x_e}$

This calculation resulted in a D_e(upper)=1.08 eV. Because the photodissociation spectrum consists of only four peaks there is a large extrapolation resulting in large error bars in D_e(upper). The excitation energy of Ni^+ can be found using Equation 5 and solving for $\Delta E(Ni^{+*} - Ni^+)$.

Equation 5: $D_0(upper) = D_0(lower) + \Delta E(Ni^{+*} - Ni^+) - T_{00}$

The $D_0(lower)$ term was determined by Armentrout and coworkers to be 1.87±.03 eV[3,4], T_{00} was found experimentally to be 2.09 eV. While $\Delta E(Ni^{+*} - Ni^+)$=1.30 eV has large uncertainty, it is still sufficient to identify the excited state of Ni^+, as Ni^+ has few excited doublet states. The nearest state is $3d^84s$, $^2F_{7/2}$ at 1.68 eV. Having identified this state, D_o(upper) can be calculated more accurately via Equation 5, using $\Delta E(Ni^{+*} - Ni^+)$=1.68 eV. The upper $Ni^+(H_2O)$ state is bound by D_0(upper)=1.46 eV. This is lower than the binding energy of the ground state, 1.87±.03 eV. The D_0 of both the upper and lower states are summarized in Figure 5.

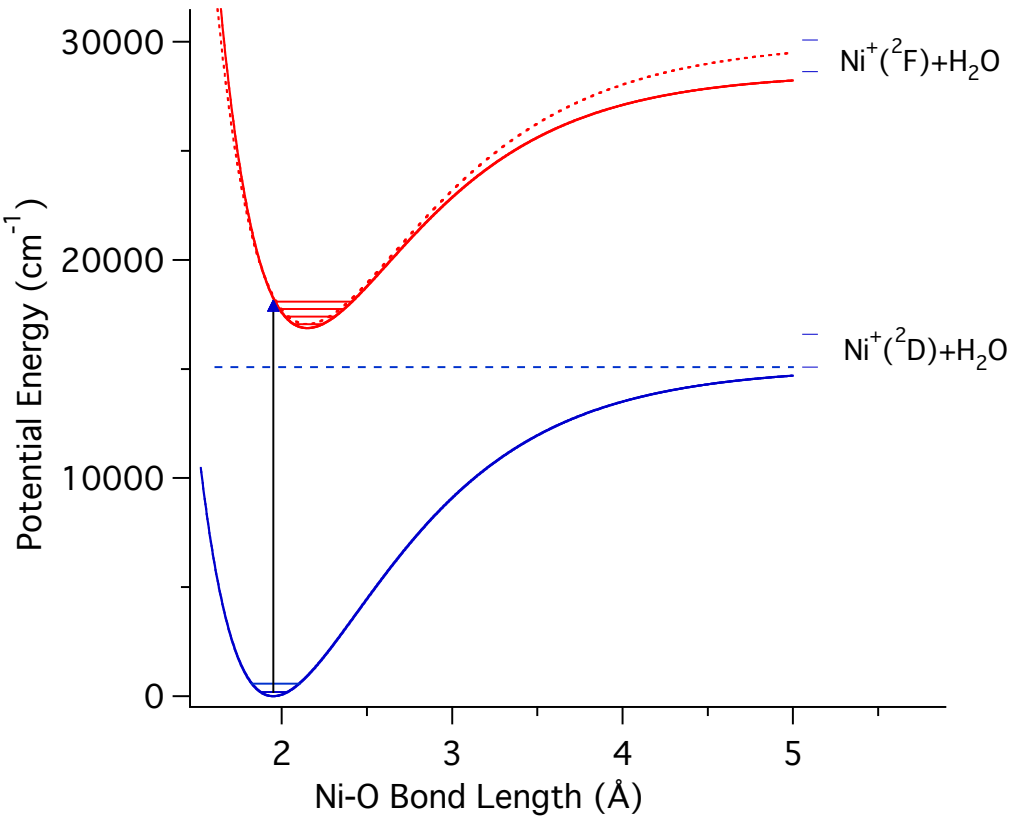

Figure 5.

$Ni^+(H_2O)$ ground state, 5th and 6th excited states, and respective potential energy surfaces. The lower blue trace is the ground state, with ^2D Ni^+ configuration and a dissociation energy indicated by the dashed red line. The D_0*(lower)* term was determined by Armentrout and coworkers to be 1.87±.03 eV[3,4]. The onset T_{00} was found experimentally to be 2.09 eV. The upper solid red trace is the 5th excited state with $^2F_{7/2}$ Ni^+ configuration. The dashed red potential directly above it is the 6th excited state's PES, which correlates to the $^2F_{5/2}$ state of Ni^+. The two blue dashes on the right indicate the 5th and 6th D_o(upper). For the 5th excited state D_o(upper)=1.46eV

Time-dependent density functional theory (TD-DFT) calculations were carried out to characterize the potential energy surfaces for the ground and excited electronic states of $Ni^+(H_2O)$ along the metal-ligand stretch coordinate (Figure 6a). These calculations use the BHandHLYP functional with the 6-311++G(3df,p) basis set. The functional reproduces the energies of excited states of bare Ni^+ very well; the B3LYP

functional underestimated excitation energies, particularly to $3d^8 4s$ states, suggesting that B3LYP overestimates that the stability of the 4s orbital relative to the 3d. Two excited states are predicted in the energy range of our study: states 5 and 6.

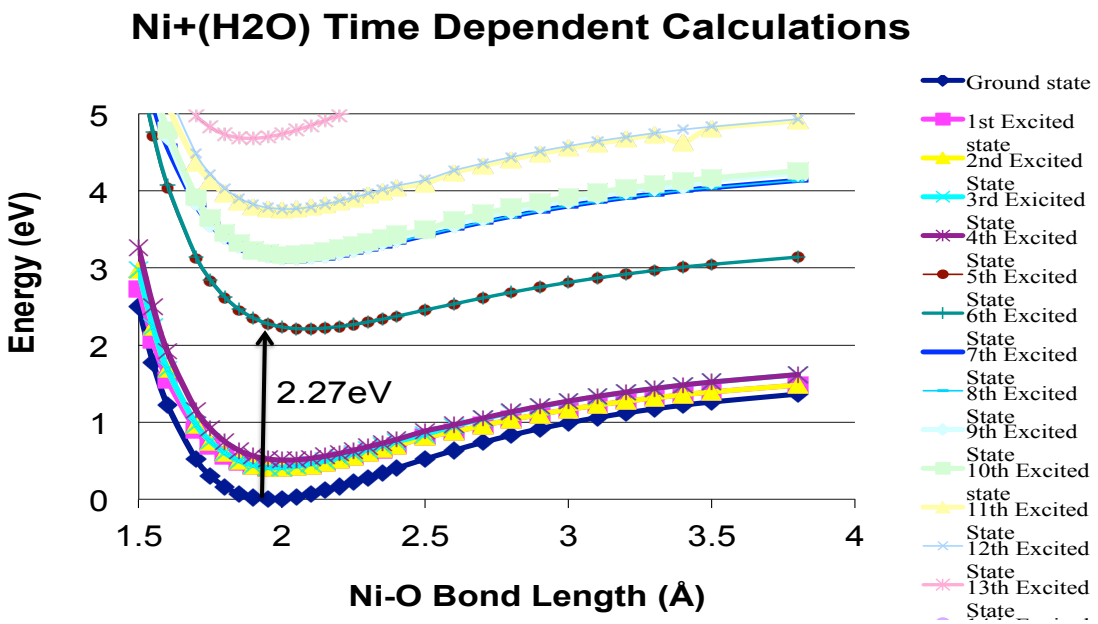

Figure 6a.

Calculated potential energy surfaces. These TD-DFT calculations used BHandHLYP/6-311G++(3df,p). The transitions that are energetically accessible are the nearly degenerate 5th and 6th states in dark green and brown. The transition occurs with ~2.27eV from the ground $^2A_1$ state to $^2A_1$ and $^2A_2$, 5th and 6th excited states, respectively. The top right corner is an orbital description of the transition occurring form the ground state to the 5th excited state.

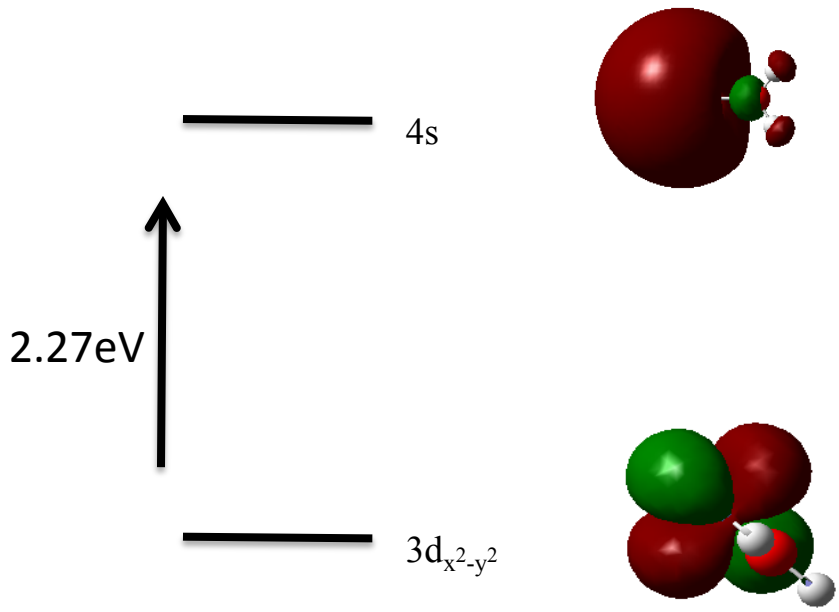

Figure 6b.
Orbital Diagram of expected transition. The 5th excited state is formed by promotion of an electron from the $3d_{x^2-y^2}$ orbital to the 4s orbital on Ni^+.

The calculations predict that the 5th and 6th excited states are nearly degenerate. They correspond to transitions from d_{xy} and $d_{x^2-y^2}$ non-bonding orbitals to a 4s orbital on the metal. The d_{xy} and $d_{x^2-y^2}$ orbitals would be identical if one ignores the hydrogens, they are very nearly degenerate as they have δ symmetry and do not participate in bonding. It also predicts that the transition from the ground state to the 5th excited state would be more intense and is a parallel transition. Transitions to the 6th electronic state are predicted to have zero intensity, as this is a $^2A_2$ state. However, the out-of-plane frequency is very low, and this transition is allowed with out-of-plane displacement.

The Ni^+-O stretching frequency was observed experimentally to be 340 cm^{-1} from the photodissociation spectrum. In between the vibrational progressions there are single peaks spaced by 340 cm^{-1} (also shown in Figure 2). It is possible that these peaks

are also vibrational progressions but of a different electronic state, perhaps the 6th excited state. Because the 5th and 6th electronic states are practically degenerate it may be that the parallel transition is occurring as the weaker progression of peaks.

The 5th and 6th excited states of $Ni^+(H_2O)$ correlate to Ni^+ states with an electron configuration of $3d^84s^1$. The ^2F is the most reasonable term assignment because it maintains the proper spin multiplicity and is in good accordance with the observed transition energy.

Intensities in the vibrational progression reflect the change in the Ni-OH_2 bond length on electronic excitation. These intensities can be calculated by solving the one-dimensional Schrodinger Equation along the Ni-O stretch coordinate. The molecule is treated as a pseudo diatomic, with the H_2O as a single "atom" with mass 18 amu. If this is done using the calculated TD-DFT potentials we obtain vibrational frequency w_e=337 cm^{-1} and w_ex_e=3.9 cm^{-1} for state 5, in good accord with experiment (Table 3). However, the calculated intensities (Frank-Condon factors) are too small for v≥2 and too large for v=0, indicating that the TD-DFT calculation underestimates the change in the Ni-O bond lengths, $\Delta r_{Ni\text{-}O}$. To determine $\Delta r_{Ni\text{-}O}$ from the experimental intensities we model the ground electronic state as a Morse oscillator with the BHandHLYP vibrational frequency and experimental dissociation energy. For the excited state, we use a Morse oscillator with the experimental frequency and dissociation energy, then vary $\Delta r_{Ni\text{-}O}$ until the best match is found between the calculated and measured intensities. This corresponds to a change in the metal-ligand bond length $\Delta r_{Ni\text{-}O}$=0.20 ± 0.02 Å. The TD-DFT calculations predict $\Delta r_{Ni\text{-}O}$ =0.15 Å, found in Table 4.

	Ni-O Bond Length (Å)	Δr_{Ni-O} (Å)
Experimental Ni^{+}-O	-	.20
Experimental Ni^{+*}-O	-	
Calculated Ni^{+}-O	1.95	.15
Calculated Ni^{+*}-O	2.10	

Table 4.

Experimental and calculated Ni-O bond lengths for the ground (Ni^{+}-O) and excited (Ni^{+*}-O) states. The experimental Δr_{Ni-O} was found by using the experimental intensities and modeling the ground electronic state as a Morse oscillator with the BHandHLYP vibrational frequency and experimental dissociation energy. To determine the excited state Δr_{Ni*-O}, a Morse oscillator is used with the experimental frequency and dissociation energy and Δr_{Ni*-O} is varied until the best match is found between the calculated and experimental intensityes.

4.3 Electronic Spectroscopy- Rotational Structure

The rotational structure in the electronic spectrum reflects rotational constants (and hence the geometry) and spin-rotational interaction of the ground and excited electronic states of $Ni^{+}(H_2O)$. Figure 7 focuses on the 1=v'←0=v'', region of the electronic spectrum and reveals the partially resolved rotational structure. The three major peaks are labeled by the K quantum numbers. The structure within each peak is due to rotations about the B and C axis (J quantum number) and to spin-rotation interaction, ε.

Because the two H atoms in $Ni^{+}(H_2O)$ can be interchanged by applying a C_2 rotation along the symmetry *a* axis it is important to employ nuclear spin statistics to attain proper K state population. For a molecule with C_{2v} geometry and two equivalent protons the nuclear spin statistics is a 3:1 degeneracy for states with overall odd:even spatial symmetry. The overall spatial symmetry is a product of the electronic, vibrational, and rotational wavefunctions.[16] The DFT calculation performed on this molecule predicts that the ground state is $^2A_1$, this can be seen in the orbital diagrams in Figure 6b.

For states with A symmetry the electronic wavefunction is totally symmetrical upon rotation about the *a* axis. The vibrational wavefunction is symmetrical for the ground vibrational state. The rotational wavefunction has even symmetry for states with K'' even and odd symmetry for states with K'' odd. Thus, overall, odd K states should be three times as intense as even states. Weights of 3:1 (odd:even) were incorporated in the simulations. At the temperature of the molecular beam, molecules are cooled to K''=0 and 1. Further cooling, from K''=1 to 0 is very inefficient, as it involves changing nuclear spin. The increased intensities for the K'=0 ←K''=1 and K'=2←K''=1 features more closely mimic those in the experiments, confirming that the ground electronic state has A symmetry.

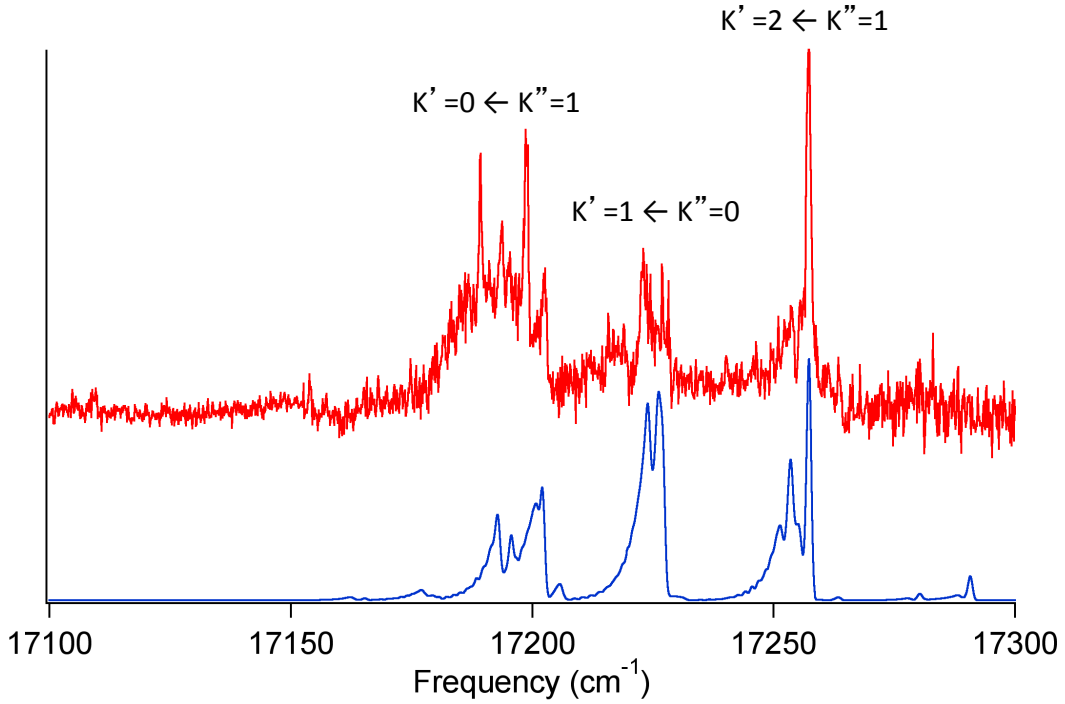

Figure 7.
Rotational simulation in the electronic spectrum. The v'=1 ←v"=0 band of $Ni^+(H_2O)$ and the simulated spectrum were determined using *spfit* and *spcat*. [15] The experimental electronic spectrum consists of perpendicular bands, showing K-type rotational structure.

The rotational structure was fit using the *spfit* and *spcat* programs.[15] The temperature and ground state A'' rotational constants were initially set at values determined in the vibrational depletion experiments. The B'' and C'' constants were fixed at the values from the hybrid density functional calculation. For the excited state, B' and C' were based on the change in Ni-O bond determined by fitting intensities in the vibrational progression.

The ground state rotational constant A'' was determined to be 13.83 cm^{-1}, using this parameter allowed for the best fit for the spectrum. Unlike the A constant in the vibrational spectrum, the excited state rotational A constant in the electronic spectrum noticeably changes relative to the ground state to A'=14.39 cm^{-1}.

The rotational constant B primarily depends on the Ni^{+}-O bond length. So, it can be expected that if the M^{+}-O bond length increases upon electronic excitation, the B rotational constant will decrease, which is the case for $Ni^{+}(H_2O)$. The DFT calculations predict that the Ni^{+}-O bond length is 1.95 Å in the ground electronic state. The Franck-Condon simulations predict that electronic excitation leads to a 0.20 Å increase in the Ni^{+}-O bond, to 2.15 Å, Table 4. This geometry was used to derive the B and C constants shown in Table 5, which were not optimized in the fit.

Rotational Constants	Experimental (cm^{-1})		Calculated (cm^{-1})	
	Ground Electronic State	**Excited Electronic State**	**Ground Electronic State**	**Excited Electronic State**
A	13.58	14.39	13.98	14.0
B	0.29	0.26	0.297	0.249
C	0.29	0.26	0.296	0.244

Table 5.

Rotational constants for the ground and excited electronic states of $Ni^+(H_2O)$. The calculated rotational constants were determined using DFT calculations at the BHandHLYP/6-311++G(3df,p) level. The experimental rotational constants were determined using *spfit* and *spcat* to simulate the rotational structure in the vibrational and electronic spectrum.[15]

The spin-rotation interaction parameter ε is due to two effects: 1) coupling of the electron spin to the magnetic field due to the rotation of the molecule and 2) second-order interaction between the spin-orbit coupling and the Coriolis interaction.[17]. The second term dominates. Although ε is rigorously a tensor and should have components along each rotational axis and each pair of axes, ε_{aa} is much larger than the other components, as the A constant is much larger than B or C, so we ignore the other components and use $\varepsilon = \varepsilon_{aa}$. The spin-orbit splitting is ~1500 cm^{-1} for the ^2D ground state and ^2F excited states of Ni^+. This large spin-orbit coupling leads to fairly large ε constants, which are responsible for much of the breadth of the K'=0←K''=1 peak.

CHAPTER 5

SUMMARY AND CONCLUSIONS

In this study the electronic spectrum of $Ni^+(H_2O)$ and its vibrational spectrum in the O-H stretching region were measured using photodissociation. The O-H stretches are observed at 3627 cm^{-1} for the symmetric stretch and 3692 cm^{-1} for the antisymmetric stretch. This corresponds to a 30 cm^{-1} shift for the symmetric stretch and 58 cm^{-1} for the antisymmetric stretch, relative to bare H_2O. Rotational analysis also shows that binding to the metal increases the H-O-H angle, due to removing electron density from the oxygen lone pair. The electronic spectrum of $Ni^+(H_2O)$ in the 550-630 nm region shows transitions to one and perhaps two electronic states. The photodissociation onset gives an upper limit to the Ni^+-H_2O bond strength of 2.09 eV, consistent with the guided ion beam value of $D_o(Ni^+\text{-}H_2O)$= 1.87±0.03 eV[3,4]. The electronic spectrum shows a long progression in the excited state metal-ligand stretch, with w_e=354.5 cm^{-1} and w_ex_e=3.6 cm^{-1}.

The ground state of $Ni^+(H_2O)$ is formed by attachment of water to ground state Ni^+ ($3d^9$, ^2D). The excited electronic state observed here correlates to $Ni^{+*}(3d^8, {}^2F)$ + H_2O. Electronic excitation involves promoting a 3d electron to the 4s orbital. The 4s orbital is larger and the promotion increases the repulsion between the metal and the oxygen lone pair. As a result, the $3d^84s$ state of Ni^+ binds H_2O less strongly than the ground $3d^9$ state. This is reflected in the reduced bond strength (1.46 eV vs. 1.87 eV), an increase in the Ni-O bond length of 0.20 Å and a relaxation of the H-O-H bond angle towards its value in bare H_2O, seen in Table 3.

CHAPTER 6

FUTURE WORK

To determine if the additional sharp peaks are indeed a result of another electronic state experiments with isotopic exchange will performed. The current experiments were all performed on $^{58}Ni^{+}(H_2O)$. I will also measure the electronic photodissociation spectrum of $^{60}Ni^{+}(H_2O)$ to confirm vibrational numbering. This experiment will also be repeated with $^{58}Ni^{+}(D_2O)$ and $^{58}Ni^{+}(HOD)$ and an isotopic shift should be observed. If the mid-peak is not another electronic state, but rather just a combination or hot band involving the in-plane or out-of plane bend, deuteration will lead to a large shift in the peak positions because these vibrations are highly sensitive to mass.

BIBLIOGRAPHY

(1) Jabri, E.; Carr, M. B.; Hausinger, R. P.; Karplus, P. A. *Science* **1995**, *268*, 998.

(2) Dixon, N. E.; Riddles, P. W.; Gazzola, C.; Blakeley, R. L.; Zerner, B. *Can. J. Biochem.* **1980**, *58*, 1335.

(3) Dalleska, N. F.; Honma, K.; Sunderlin, L. S.; Armentrout, P. B. *J. Am. Chem. Soc.* **1994**, *116*, 3519.

(4) Armentrout, P. B.; Kickel, B. L. Gas-Phase Thermochemistry of Transition Metal Ligand Systems: Reassessment of Values and Periodic Trends. In *Organometallic Ion Chemistry*; Freiser, B. S., Ed.; Kluwer Academic Publishers: Dordrecht, The Netherlands, 1994; pp 1.

(5) Lessen, D.; Brucat, P. J. *Chem. Phys. Lett.* **1988**, *152*, 473.

(6) Asher, R. L.; Bellert, D.; Buthelezi, T.; Brucat, P. J. *Chem. Phys. Lett.* **1994**, *228*, 599.

(7) Bellert, D.; Buthelezi, T.; Lewis, V.; Dezfulian, K.; Brucat, P. J. *Chem. Phys. Lett.* **1995**, *240*, 495.

(8) Asher, R. L.; Bellert, D.; Buthelezi, T.; Weerasekera, G.; Brucat, P. J. *Chem. Phys. Lett.* **1994**, *228*, 390.

(9) Walters, R. S.; Pillai, E. D.; Duncan, M. A. *J. Am. Chem. Soc.* **2005**, *127*, 16599.

(10) Crim, F. F. *Annu. Rev. Phys. Chem.* **1993**, *44*, 397.

(11) Citir, M.; Altinay, G.; Metz, R. B. *J. Phys. Chem. A* **2006**, *110*, 5051.

(12) Wiley, W. C.; McLaren, I. H. *Rev. Sci. Instrum.* **1955**, *26*, 1150.

(13) Carnegie, P. D.; Bandyopadhyay, B.; Duncan, M. A. *J. Phys. Chem. A* **2008**, *112*, 6237.

(14) Kocak, A.; Austein-Miller, G.; Altinay, G.; Metz, R. B. *to be submitted* **2011**.

(15) Pickett, H. M. *J. Mol. Spectrosc.* **1991**, *148*, 371.

(16) Ellis, A. M.; Feher, M.; Wright, T. G. *Electronic and Photoelectron Spectroscopy: Fundamentals and Case Studies*; Cambridge University Press: Cambridge, UK, 2005.

(17) Tarczay, G.; Gopalakrishnan, S.; Miller, T. A. *J. Mol. Spectrosc.* **2003**, *220*, 276.